Glassy Phase of Optimal Quantum Control

Alexandre G. R. Day,[1,*] Marin Bukov,[2,†] Phillip Weinberg,[1] Pankaj Mehta,[1] and Dries Sels[1,3,4]

[1] *Department of Physics, Boston University, 590 Commonwealth Avenue, Boston, Massachusetts 02215, USA*

[2] *Department of Physics, University of California, Berkeley, California 94720, USA*

[3] *Department of Physics, Harvard University, 17 Oxford Street, Cambridge, Massachusetts 02138, USA*

[4] *Theory of Quantum and Complex Systems, Universiteit Antwerpen, B-2610 Antwerpen, Belgium*

(Received 27 July 2018; published 15 January 2019)

We study the problem of preparing a quantum many-body system from an initial to a target state by optimizing the fidelity over the family of bang-bang protocols. We present compelling numerical evidence for a universal spin-glasslike transition controlled by the protocol time duration. The glassy critical point is marked by a proliferation of protocols with close-to-optimal fidelity and with a true optimum that appears exponentially difficult to locate. Using a machine learning (ML) inspired framework based on the manifold learning algorithm *t*-distributed stochastic neighbor embedding, we are able to visualize the geometry of the high-dimensional control landscape in an effective low-dimensional representation. Across the transition, the control landscape features an exponential number of clusters separated by extensive barriers, which bears a strong resemblance with replica symmetry breaking in spin glasses and random satisfiability problems. We further show that the quantum control landscape maps onto a disorder-free classical Ising model with frustrated nonlocal, multibody interactions. Our work highlights an intricate but unexpected connection between optimal quantum control and spin glass physics, and shows how tools from ML can be used to visualize and understand glassy optimization landscapes.

DOI: 10.1103/PhysRevLett.122.020601

State preparation plays a quintessential role in present-day studies of quantum physics. The ability to reliably manipulate and control quantum states has proven crucial to many physical systems, from quantum mechanical emulators ultracold atoms [1–3] and trapped ions [4–6], through solid-state systems like superconducting qubits [7], to nitrogen-vacancy centers [8]. The nonequilibrium character of quantum state manipulation makes it a difficult and not well-understood problem of ever-increasing importance to building a large-scale quantum computer [9].

Analytically, state preparation has been studied using both adiabatic perturbation theory [10] and shortcuts to adiabaticity [11–15]. Unfortunately, these theories have limited application in nonintegrable many-body systems, for which no exact closed-form expressions can be obtained. This has motivated the development of efficient numerical algorithms, such as GRAPE [16,17], CRAB [18], and Machine learning based approaches [19–31]. State preparation can be formulated as an optimal control problem for which the objective is to find the set of controls that extremize a cost function, i.e., determine the optimal fidelity to prepare a target state, subject to physical and dynamical constraints. However, cost functions are usually defined on a high-dimensional space and are typically nonconvex. For this reason, sophisticated algorithms must be devised to guarantee finding the global optimum. Moreover, optimality does not automatically imply stability and robustness of the solution, which are required for experimental applications. Establishing the general limitations and constraints of quantum control is crucial for guiding the field forward.

Recently, it was shown that the quantum state preparation paradigm supports a number of *control phase transitions* by varying the protocol duration T [22,32,33], exhibiting overconstrained, controllable, correlated, and glassy phases. Glasslike systems are expected to feature slow equilibration timescales related to an underlying extremely rugged free-energy landscape. Such features have been extensively discussed in the context of spin-glass physics [34–37] and in hard combinatorial [38–41] and random satisfiability [42–48] problems.

In this work we provide evidence for the existence of a generic glasslike control phase transition observed in the manipulation of generic nonintegrable spin chains with a single global control field. By sampling the optimization landscape for this state preparation problem, we discover the existence of a glasslike critical point marked by an extremely rugged landscape with an exponential number local extrema. This transition in the control landscape is visualized using the manifold learning method known as t-distributed stochastic neighbor embedding (t-SNE) [49], which reveals the clustering of minima near the glass transition. We further present a mapping of this dynamical optimal control problem to a *static* frustrated classical spin model with all-to-all multibody interactions, the energy landscape of which is in one-to-one correspondence with the original optimization landscape. Similar to the problem of finding the ground-state of spin glasses, we find strong evidence for an exponential algorithmic complexity scaling in the number of *control* degrees of freedom for the task of locating the optimal protocol, suggesting that quantum state preparation is nondeterministic polynomial time-complete in the glassy phase.

Problem setup.—Consider a periodic chain of L interacting qubits (Pauli operator S_i^μ), controlled by a global time-dependent transverse-field:

$$H(t) = -\sum_{i=1}^{L} J S_{i+1}^z S_i^z + g S_i^z + h(t) S_i^x, \tag{1}$$

with interaction strength $J = 1$ (sets the energy scale), and an external magnetic field of a static z component $g = 1$ and a time-varying x component $h(t)$. The presence of the longitudinal z field renders the model nonintegrable at any fixed time t, with no known closed-form expression for the exact instantaneous eigenstates and eigenenergies. We work in a nonperturbative regime with all couplings of similar magnitude, and choose a bounded control $|h(t)| \le 4$ reflecting the experimental infeasibility to inject unlimited amounts of energy in the system.

The system is prepared at $t = 0$ in the paramagnetic ground state (GS) $|\psi_i\rangle$ of $H[h = -2]$. Our goal is to find a protocol $h^*(t)$ which, following Schrödinger evolution for a fixed short duration $T \in [0, 4]$, brings the initial state $|\psi_i\rangle$ as close as possible to the target state—the paramagnetic GS $|\psi_*\rangle$ of $H[h = +2]$, as measured by the many-body fidelity $F_h(T) = |\langle\psi_*|\psi(T)\rangle|^2$. The specific values of the field for the initial and target states, $h = \pm 2$, were chosen to be of similar magnitude as the interaction strength $J = 1$. We checked that the conclusions we draw in this work are insensitive to this choice.

Whether preparing the target state with unit fidelity is feasible in the thermodynamic (TD) limit $L \to \infty$ is currently an open question related to the existence of a finite quantum speed limit [15,50,51]. Let us formulate this objective as a minimization problem, and choose as a cost function the (negative) log-fidelity $C_h(T) = -\log F_h(T)/L$. $C_h(T)$ remains intensive in the TD limit, and we verified that our results do not change qualitatively starting from $L \ge 6$ [52]. Thus, the emerging log-fidelity landscape $h(t) \mapsto C_h(T)$ corresponds to the control landscape for quantum state preparation [16,53,54] [Fig. 1(c)]. The optimal protocol $h^*(t)$ is defined as the global minimum of the log-fidelity landscape. We divide the protocol duration $T = \delta t N_T$ into N_T steps of size δt. We are interested in the properties of the control landscape in the large N_T limit. Motivated by Pontryagin's maximum principle and the optimal control literature, we restrict the discussion to bang-bang protocols [Fig. 1(a)] where the control field can take only the maximum allowed values $h(t) \in \{\pm 4\}$ at each time step [55,56].

Control landscape and sampling method.—In general, the control landscape $C_h(T)$ is a nonconvex functional

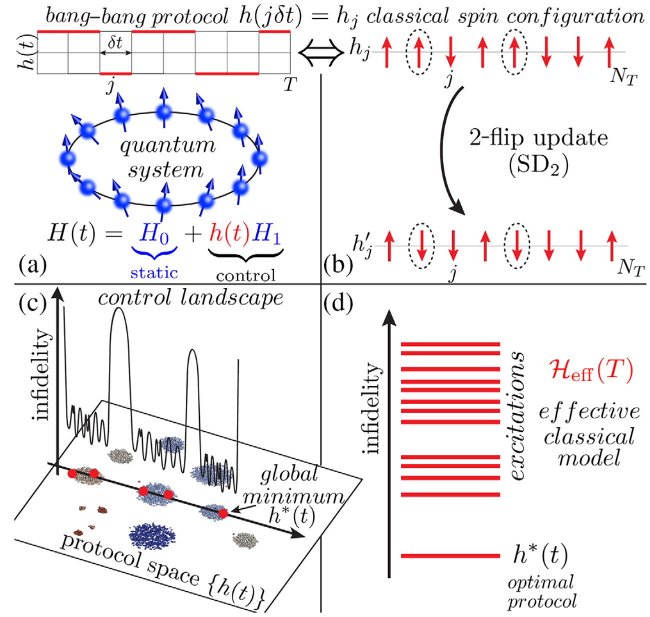

FIG. 1. Bang-bang protocols $h(j\delta t)$ to control a quantum system with high fidelity (a) are equivalent to classical spin configurations h_j with log fidelity playing the role of energy. (b) Using k-flip stochastic descent, we explore the log-fidelity landscape (c), and find a glasslike transition in the control landscape described by the effective classical model $\mathcal{H}_{\rm eff}$ (d).

of $h(t)$: local minima obtained using a greedy optimization approach depend on the initial starting points of the algorithm. Using stochastic descent (SD) [52], we start from a random protocol and flip the sign of $h(j\delta t)$ at k different time steps $j_1, \ldots, j_k$ chosen uniformly at random [Fig. 1(b)]. A set of flips is accepted only if it decreases $C_h(T)$. We repeat this process until a local minimum is reached (see Supplemental Material [52] for psuedocode). A protocol $h(t)$ is a SD$_k$ local minimum if *all* possible k-flip updates increase the log fidelity. We use SD$_k$ algorithms with $k = 1$, $k = 2$, and $k = 4$ flips per local update. The best found fidelity $F_h(T)$ as a function of protocol duration is presented in Fig. 2 (black line).

Order parameters measured.—The structure of the control landscape can be understood by measuring the protocol correlator and the number of unique local minima which we now define. Consider the set $\mathcal{S} = \{h^\alpha(t)\}$ of all local log-fidelity minima. We sample M protocols from $\mathcal{S}$ using SD$_k$ and denote $\bar{h}(t) \equiv M^{-1}\sum_{\alpha=1}^{M} h^\alpha(t)$ as the sample average. Let us define the protocol correlator:

$$q_{{\rm SD}_k}(T) = \frac{1}{16 N_T} \sum_{j=1}^{N_T} \overline{\{h(j\delta t) - \bar{h}(j\delta t)\}^2}, \tag{2}$$

which is related to the Edwards-Anderson order parameter for replica symmetry breaking in spin glasses [57–59]. If the landscape is convex (unique minimum), $q = 0$; while if all the sampled local minima are uncorrelated, $q = 1$.

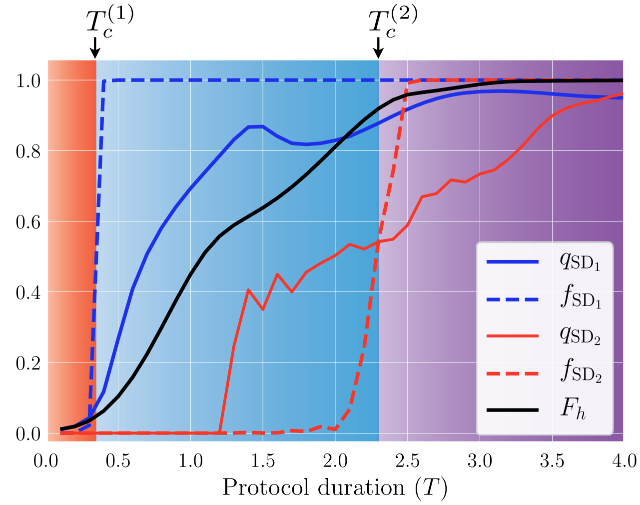

FIG. 2. Preparing states in a chain of qubits with optimal many-body fidelity $F_h(T)$ (black) features transitions from an overconstrained phase (red region) to a correlated phase (blue region) to a glasslike phase (purple region) at protocol durations $T_c^{(1)}$ and $T_c^{(2)}$. This is revealed by the nonzero fraction $f_{\mathrm{SD}_k}(T)$ order parameter. We used k-flip stochastic descent (SD_k) on the family of bang-bang protocols with $N_T = 200$, $L = 6$ and $M = 10^5$.

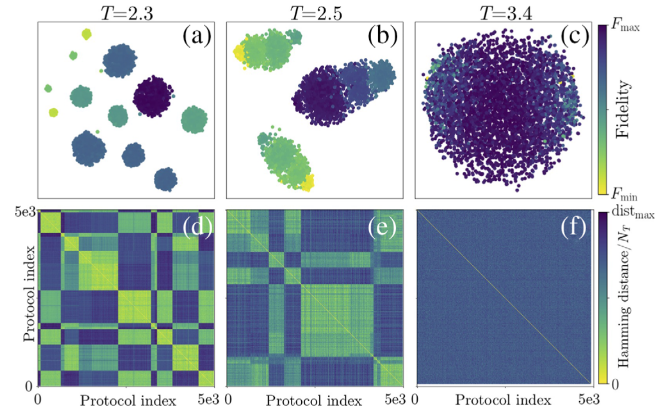

FIG. 3. (a)–(c) t-SNE visualization of the control landscape above the SD_2 glass critical point $T_c^{(2)} \approx 2.3$. Each data point represents a local $C_h(T)$ minimum—a bang-bang protocol embedded in a two-dimensional t-SNE space. Embedded protocols are colored by their fidelity in the interval $[F_{\min}, F_{\max}]$ with intervals [0.919, 0.920], [0.958, 0.959], [0.992, 0.997] from (a) to (c). (a),(b) The local minima cluster are separated by extensive barriers as seen in (d),(e), the Hamming distance matrix for the local-minima protocols. $\mathrm{dist}_{\max} = 0.5$, 0.52, 0.61 for (d),(e),(f), respectively. The protocols in the Hamming matrix are grouped by their cluster index found using density clustering (see Supplemental Material [52]). (c) At larger protocol duration ($T = 3.4$) large clusters fracture in an exponential number of small clusters. The small clusters are separated by extensive barriers (f). We used SD_2 with $N_T = 200$, $L = 6$ and sampled 5000 unique protocols.

In collecting M samples, we denote $M^\star \leq M$ as the number of distinct protocols. We further define the fraction of distinct local minima as

$$f_{\mathrm{SD}_k} \equiv M^\star / M. \tag{3}$$

For a fixed number of samples, this fraction is sensitive to drastic changes in the number of distinct local minima in $\mathcal{S}$.

Overconstrained and correlated phases.— The correlator q_{SD_1} as a function of the protocol duration T is shown in Fig. 2. For $T < T_c^{(1)} \approx 0.35$, $f_{\mathrm{SD}_1} = 1/M$, and the log-fidelity landscape is convex. While the maximum attainable fidelity is small, there exists a unique optimal protocol which is easy to find using SD_1. At $T = T_c^{(1)}$, the control landscape undergoes a phase transition from an overconstrained phase ($q_{\mathrm{SD}_1} = 0$, red region) to a correlated phase ($q_{\mathrm{SD}_1} > 0$, blue region). This transition is characterized by a rapid increase of the number of quasidegenerate SD_1 local minima as shown by f_{SD_1} reaching unity for $T > T_c^{(1)}$. However, these local minima are all separated by barriers of width 2 in Hamming distance (number of sign flips required to connect them). This is revealed by using SD_2 just above $T_c^{(1)}$, for which $f_{\mathrm{SD}_2} = 1/M$ and $q_{\mathrm{SD}_2} = 0$. At $T \approx 1.2$, q_{SD_2} becomes nonzero, indicating the appearance of multiple SD_2 local minima. However, the unique fraction of those minima f_{SD_2} remains nearly zero. Remarkably, the control landscape undergoes another transition at $T_c^{(2)} \approx 2.3$, characterized by a proliferation of SD_2 local minima, where $f_{\mathrm{SD}_2} \sim \mathcal{O}(1)$.

Glassy phase.— To better understand the physics behind this SD_2 glassy transition, we visualize the log-fidelity landscape using the nonlinear-manifold machine learning method t-distributed stochastic neighbor-embedding [49] (Fig. 3). t-SNE embeddings preserve local ordination of data, and hence allow us to understand the geometry of the control landscape. At $T_c^{(2)}$, the geometry of the control landscape undergoes a drastic transition with the appearance of distinct clusters in the space of near-optimal protocols (see Fig. 3 and Supplemental Material [52] for clustering procedure). Each cluster corresponds to a distinct region of closely related SD_2 minima. While protocols *within* a cluster are similar and connected by small barrier widths, protocols *between* clusters are separated by barriers of width *extensive* in N_T [52]. At longer protocol durations $T \gtrsim 3.0$ [Figs. 3(c)–3(f)], the number of clusters appears to be exponential in N_T and all protocols are separated by extensive barriers (Fig. 3(f) and see Supplemental Material [52]). The number of SD_k local minima is large, $f_{\mathrm{SD}_k} \to 1$, and we find that it scales exponentially with N_T [52]. Therefore, we expect that any local-flip algorithm (e.g., SD_k with k subextensive in N_T) will have exponential run time for finding the global optimum. Having a landscape with an exponential number of minima separated by extensive barriers (in height and width) in the number of degrees of freedom is one of the landmarks of spin glasses, and leads to extremely slow mixing times [35].

This glassy control transition is analogous to replica symmetry breaking in spin glasses and random satisfiability problems [60,61]. We verified that applying higher-order SD_k ($k > 2$) only slightly shifts the glass critical point to larger T, as expected due to the presence of large and numerous barriers [52].

Effective classical model.—To further evidence the glassy character of the phase, we map the control problem to an effective classical Ising model $\mathcal{H}_{\rm eff}(T)$, which governs the control landscape phase transitions. By studying its properties, we establish a closer connection with spin glasses. Similar to classical Ising-type models, in which each spin configuration comes with its energy, we assign to every bang-bang protocol the log-fidelity $C_h(T)$ of being in the target state [Fig. 1(d)]. From the set of all $C_h(T)$ values, which we refer to as the log-fidelity "spectrum," we reconstruct an effective classical spin model:

$$\mathcal{H}_{\rm eff}(T) = C_0(T) + \sum_{j=1}^{N_T} G_j(T)h_j + \frac{1}{N_T}\sum_{i\neq j}^{N_T} J_{ij}(T)h_ih_j + \frac{1}{N_T^2}\sum_{i\neq j\neq k}^{N_T} K_{ijk}(T)h_jh_jh_k + \dots. \tag{4}$$

Here the couplings G_j, J_{ij}, K_{ijk}, which can be uniquely computed by tracing over all 2^{N_T} possible protocol configurations [52], encode all the information about the control landscape [52].

For $T > T_1^{(c)}$, we find that the effective two-body interaction J_{ij} (which is nonlocal and antiferromagnetic) and the one-body interaction compete, resulting in $\mathcal{H}_{\rm eff}(T)$ being highly frustrated; i.e., a large fraction of the J_{ij} bonds are unsatisfied in the ground state [52]. For larger times, higher-order (and possibly all) nonlocal multibody spin interactions in $\mathcal{H}_{\rm eff}(T)$ are required to reliably capture the behavior of the system in the glassy phase. We present further evidence for these claims using an independent procedure for learning couplings based on the RIDGE algorithm for sparse linear regression [52,62,63]. The long-range and multibody nature of the couplings is related to the dynamic origin of the state preparation problem: causality imposes that the value of the low-$C_h(T)$ protocols at time t is correlated with the values at all previous times $t' < t$ in the bang-bang sequence.

Density of states.— In order to understand the underlying causes for the glassy phase, we examine the density of states (i.e., protocols) of $\mathcal{H}_{\rm eff}(T)$ (DOS), obtained by counting protocols in a small fidelity window (Fig. 4, black line, left axis). Starting from a protocol h^* with near-optimal fidelity [i.e., a low-energy local minimum of $\mathcal{H}_{\rm eff}(T)$], we analyze the behavior of elementary excitations [Fig. 1(d)], by computing the fidelity of all possible protocols obtained after flipping 1, 2, and 4 bangs in h^*. These excitations can be classified by their "magnetization" $M_h = \sum_j (h_j - h_j^*)$ relative to the near-optimal protocol. Below the SD_2 glass transition, $T < T_c^{(2)} \approx 2.3$, the bulk of the excitations (shaded area, right axis) is located in a region where the DOS is much smaller than the typical DOS. Therefore, when searching for the optimal protocol, starting from an initial protocol with large log fidelity, finding one of the elementary excitations is relatively easy since most of these excitations are in a region of extremely small DOS (with respect to the typical DOS). In contrast, for $T > T_c^{(2)}$ in the glassy phase, the bulk of the excitations moves to a region where the DOS is large. This implies that if we miss one of the elementary excitations in the search for a better protocol, it becomes infeasible to reach h^*. From an algorithmic perspective, this suggests a transition from a subexponential complexity to an at least exponential complexity in N_T. We explicitly verified that this behavior holds using exact numerical computation of all protocol fidelities up to $N_T \leq 28$ [52].

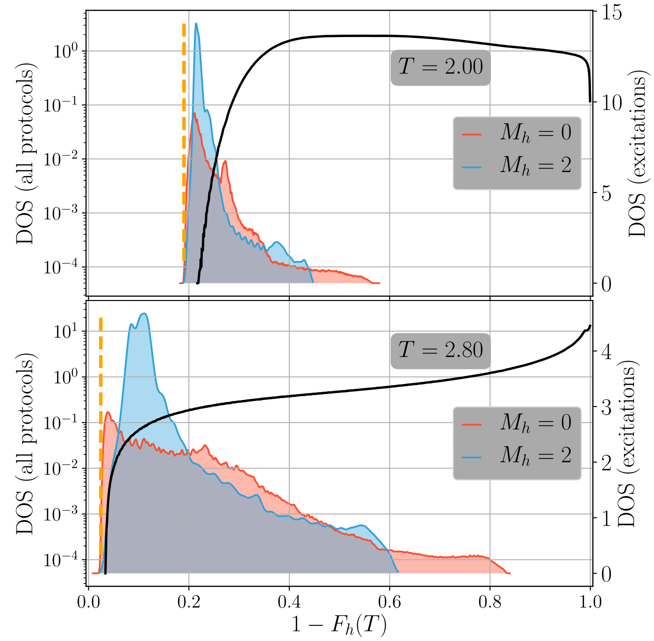

FIG. 4. Normalized density of states (DOS) of $\mathcal{H}_{\rm eff}$ (black line, left y axis), and the distribution of the $M_h = 0$ and $M_h = 2$-magnetized excitations (shaded, right y axis) on both sides of the glass critical point $T_c^{(2)} \approx 2.3$ for $N_T = 80$, $L = 6$. The position of the best obtained fidelity using SD_4 is marked by the vertical dashed line.

Outlook/discussion.— Studying the properties of the control landscape, we provided compelling evidence for the existence of a glasslike phase in optimal ground state manipulation of constrained quantum systems. Using t-SNE we were able to reveal the complex geometry of the high-dimensional control landscape, which features multiple clusters separated by extensive barriers. We mapped this out-of-equilibrium problem to an effective classical Ising model with nonlocal and frustrated multibody interactions, resulting in a complicated optimal protocol configuration. Further, applying ideas from condensed matter physics to reveal the microscopic origin of the putative glassy control phase, we analyzed the behavior of the DOS in protocol space of the distribution of local elementary excitations above the low log-fidelity manifold. Our analysis suggest that the state preparation paradigm in nonintegrable many-body systems belongs to the class of nondeterministic polynomial time-complete problems, with the optimal protocol becoming exponentially hard to find in the glass phase.

The approach outlined in this work has the potential to further the understanding of quantum dynamics away from equilibrium. It generalizes to control problems beyond state preparation, for instance minimizing work fluctuations [64], and highlights the application of machine learning and glass-physics methods to quantum control tasks.

We thank A. Polkovnikov, C. Laumann, and C. Baldwin for illuminating discussions. A. D. was supported by a NSERC. A. D. and P. M. acknowledge support from Simon's Foundation through the MMLS Fellow program. M. B. was supported by the Emergent Phenomena in Quantum Systems initiative of the Gordon and Betty Moore Foundation, the ERC synergy grant UQUAM, and the U.S. Department of Energy, Office of Science, Office of Advanced Scientific Computing Research, Quantum Algorithm Teams Program. D. S. acknowledges support of the FWO of the Research Foundation, Flanders. This research was supported in part by the National Science Foundation under Grant No. NSF PHY-1748958. We used Quspin for simulating the dynamics of the qubit system [65,66]. The authors are pleased to acknowledge that the computational work reported on in this paper was performed on the Shared Computing Cluster which is administered by Boston University's Research Computing Services.

[*]agrday@bu.edu
[†]mgbukov@berkeley.edu

[1] M. G. Bason, M. Viteau, N. Malossi, P. Huillery, E. Arimondo, D. Ciampini, R. Fazio, V. Giovannetti, R. Mannella, and O. Morsch, Nat. Phys. **8**, 147 (2012).
[2] S. van Frank, M. Bonneau, J. Schmiedmayer, S. Hild, C. Gross, M. Cheneau, I. Bloch, T. Pichler, A. Negretti, T. Calarco *et al.*, Sci. Rep. **6**, 34187 (2016).
[3] P. B. Wigley, P. J. Everitt, A. van den Hengel, J. Bastian, M. A. Sooriyabandara, G. D. McDonald, K. S. Hardman, C. Quinlivan, P. Manju, C. C. Kuhn *et al.*, Sci. Rep. **6**, 25890 (2016).
[4] R. Islam, E. E. Edwards, K. Kim, S. Korenblit, C. Noh, H. Carmichael, G.-D. Lin, L.-M. Duan, C.-C. Joseph Wang, J. K. Freericks, and C. Monroe, Nat. Commun. **2**, 377 (2011).
[5] C. Senko, P. Richerme, J. Smith, A. Lee, I. Cohen, A. Retzker, and C. Monroe, Phys. Rev. X **5**, 021026 (2015).
[6] P. Jurcevic, B. P. Lanyon, P. Hauke, C. Hempel, P. Zoller, R. Blatt, and C. F. Roos, Nature (London) **511**, 202 (2014).
[7] R. Barends, A. Shabani, L. Lamata, J. Kelly, A. Mezzacapo, U. Las Heras, R. Babbush, A. Fowler, B. Campbell, Y. Chen *et al.*, Nature (London) **534**, 222 (2016).
[8] B. B. Zhou, A. Baksic, H. Ribeiro, C. G. Yale, F. J. Heremans, P. C. Jerger, A. Auer, G. Burkard, A. A. Clerk, and D. D. Awschalom, Nat. Phys. **13**, 330 (2017).
[9] M. A. Nielsen and I. Chuang, *Quantum Computation and Quantum Information* (AAPT, 2002).
[10] M. Kolodrubetz, D. Sels, P. Mehta, and A. Polkovnikov, Phys. Rep. **697**, 1 (2017).
[11] M. Demirplak and S. A. Rice, J. Phys. Chem. A **107**, 9937 (2003).
[12] A. del Campo, Phys. Rev. Lett. **111**, 100502 (2013).
[13] C. Jarzynski, Phys. Rev. A **88**, 040101 (2013).
[14] D. Sels and A. Polkovnikov, Proc. Natl. Acad. Sci. U.S.A. **114**, E3909 (2017).
[15] M. Bukov, D. Sels, and A. Polkovnikov, arXiv:1804.05399.
[16] S. J. Glaser, T. Schulte-Herbrüggen, M. Sieveking, O. Schedletzky, N. C. Nielsen, O. W. Sørensen, and C. Griesinger, Science **280**, 421 (1998).
[17] N. Khaneja, T. Reiss, C. Kehlet, T. Schulte-Herbrueggen, and S. J. Glaser, J. Magn. Reson. **172**, 296 (2005).
[18] T. Caneva, T. Calarco, and S. Montangero, Phys. Rev. A **84**, 022326 (2011).
[19] R. S. Judson and H. Rabitz, Phys. Rev. Lett. **68**, 1500 (1992).
[20] C. Chen, D. Dong, R. Long, I. R. Petersen, and H. A. Rabitz, Phys. Rev. A **89**, 023402 (2014).
[21] C. Chen, D. Dong, H.-X. Li, J. Chu, and T.-J. Tarn, IEEE Trans. Neural Netw. Learn. Syst. **25**, 920 (2014).
[22] M. Bukov, A. G. R. Day, D. Sels, P. Weinberg, A. Polkovnikov, and P. Mehta, Phys. Rev. X **8**, 031086 (2018).
[23] X.-C. Yang, M.-H. Yung, and X. Wang, Phys. Rev. A **97**, 042324 (2018).
[24] V. Dunjko and H. J. Briegel, arXiv:1709.02779.
[25] M. August and J. M. Hernández-Lobato, arXiv:1802.04063.
[26] T. Fösel, P. Tighineanu, T. Weiss, and F. Marquardt, Phys. Rev. X **8**, 031084 (2018).
[27] J. J. Sorensen, M. Aranburu, T. Heinzel, and J. Sherson, arXiv:1802.07521.
[28] X.-M. Zhang, Z.-W. Cui, X. Wang, and M.-H. Yung, Phys. Rev. A **97**, 052333 (2018).
[29] M. Y. Niu, S. Boixo, V. Smelyanskiy, and H. Neven, arXiv:1803.01857.
[30] F. Albarrán-Arriagada, J. C. Retamal, E. Solano, and L. Lamata, Phys. Rev. A **98**, 042315 (2018).
[31] M. Bukov, Phys. Rev. B **98**, 224305 (2018).
[32] M. Bukov, A. G. R. Day, P. Weinberg, A. Polkovnikov, P. Mehta, and D. Sels, Phys. Rev. A **97**, 052114 (2018).
[33] M. Larocca, P. Poggi, and D. Wisniacki, arXiv:1802.05683.
[34] M. Mézard, G. Parisi, and M. Virasoro, *Spin Glass Theory and Beyond: An Introduction to the Replica Method and Its Applications* (World Scientific Publishing Company, Singapore, 1987), Vol. 9.

[35] H. Nishimori, *Statistical Physics of Spin Glasses and Information Processing: An Introduction* (Clarendon Press, Oxford, England, 2001), Vol. 111.
[36] D. Hu, P. Ronhovde, and Z. Nussinov, Philos. Mag. **92**, 406 (2012).
[37] V. Ros, G. Biroli, and C. Cammarota, arXiv:1809.05440.
[38] R. Monasson and R. Zecchina, Phys. Rev. E **56**, 1357 (1997).
[39] M. Leone, F. Ricci-Tersenghi, and R. Zecchina, J. Phys. A **34**, 4615 (2001).
[40] L. Zdeborová, Acta Phys. Slovaca **59**, 169 (2009).
[41] K. Klemm, A. Mehta, and P. F. Stadler, PLoS One **7**, e34780 (2012).
[42] F. Ricci-Tersenghi, M. Weigt, and R. Zecchina, Phys. Rev. E **63**, 026702 (2001).
[43] M. Mézard, G. Parisi, and R. Zecchina, Science **297**, 812 (2002).
[44] M. Mézard, in *Proceedings of the International Conference on Theoretical Physics* (Springer, New York, 2003), pp. 475–488.
[45] D. Battaglia, M. Kolář, and R. Zecchina, Phys. Rev. E **70**, 036107 (2004).
[46] M. Mézard, M. Palassini, and O. Rivoire, Phys. Rev. Lett. **95**, 200202 (2005).
[47] D. Hu, P. Ronhovde, and Z. Nussinov, Phys. Rev. E **86**, 066106 (2012).
[48] S. C. Morampudi, B. Hsu, S. L. Sondhi, R. Moessner, and C. R. Laumann, Phys. Rev. A **96**, 042303 (2017).
[49] L. v. d. Maaten and G. Hinton, J. Mach. Learn. Res. **9**, 2579 (2008).
[50] V. Jurdjevic and H. J. Sussmann, J. Differ. Equations **12**, 313 (1972).
[51] T. Caneva, A. Silva, R. Fazio, S. Lloyd, T. Calarco, and S. Montangero, Phys. Rev. A **89**, 042322 (2014).
[52] See Supplemental Material at http://link.aps.org/supplemental/10.1103/PhysRevLett.122.020601 for details about the stochastic descent algorithm, its implementation and comparisons for various parameters (number of flips, number of bangs allowed, etc.), discussion about clustering and the methods used to identify the clusters, and finally, it contains more details concerning the fitted couplings using the effective Ising Hamiltonian.
[53] H. A. Rabitz, M. M. Hsieh, and C. M. Rosenthal, Science **303**, 1998 (2004).
[54] K. W. Moore and H. Rabitz, J. Chem. Phys. **137**, 134113 (2012).
[55] Z.-C. Yang, A. Rahmani, A. Shabani, H. Neven, and C. Chamon, Phys. Rev. X **7**, 021027 (2017).
[56] S. Bao, S. Kleer, R. Wang, and A. Rahmani, Phys. Rev. A **97**, 062343 (2018).
[57] G. Parisi, Phys. Rev. Lett. **50**, 1946 (1983).
[58] T. Castellani and A. Cavagna, J. Stat. Mech. 2005, P05012 (2005).
[59] L. O. Hedges, R. L. Jack, J. P. Garrahan, and D. Chandler, Science **323**, 1309 (2009).
[60] M. Mezard and A. Montanari, *Information, Physics, and Computation* (Oxford University Press, Oxford, England, 2009).
[61] C. Moore and S. Mertens, *The Nature of Computation* (Oxford University Press, Oxford, England, 2011).
[62] P. Mehta, M. Bukov, C. H. Wang, A. G. R. Day, C. Richardson, C. K. Fisher, and D. J. Schwab, arXiv:1803.08823.
[63] J. Friedman, T. Hastie, and R. Tibshirani, *The Elements of Statistical Learning*, Springer Series in Statistics (Springer, New York, 2001), Vol. 1.
[64] A. P. Solon and J. M. Horowitz, Phys. Rev. Lett. **120**, 180605 (2018).
[65] P. Weinberg and M. Bukov, SciPost Phys. **2**, 003 (2017).
[66] P. Weinberg and M. Bukov, arXiv:1804.06782.